European Journal of Nuclear Medicine and Molecular Imaging (2019) 46:280–287
https://doi.org/10.1007/s00259-018-4182-1

ORIGINAL ARTICLE

Amyloid PET as a marker of normal-appearing white matter early damage in multiple sclerosis: correlation with CSF β-amyloid levels and brain volumes

Anna M. Pietroboni[1,2,3] · Tiziana Carandini[1,2,3] · Annalisa Colombi[1,2,3] · Matteo Mercurio[1] · Laura Ghezzi[1,2,3] · Giovanni Giulietti[4] · Marta Scarioni[1,2,3] · Andrea Arighi[1,2,3] · Chiara Fenoglio[2] · Milena A. De Riz[1,2,3] · Giorgio G. Fumagalli[1,2,3,5] · Paola Basilico[1,2,3] · Maria Serpente[2] · Marco Bozzali[4,6] · Elio Scarpini[1,2,3] · Daniela Galimberti[1,2,3] · Giorgio Marotta[1,2]

Received: 24 July 2018 / Accepted: 25 September 2018 / Published online: 21 October 2018

Abstract

Purpose The disease course of multiple sclerosis (MS) is unpredictable, and reliable prognostic biomarkers are needed. Positron emission tomography (PET) with β-amyloid tracers is a promising tool for evaluating white matter (WM) damage and repair. Our aim was to investigate amyloid uptake in damaged (DWM) and normal-appearing WM (NAWM) of MS patients, and to evaluate possible correlations between cerebrospinal fluid (CSF) β-amyloid$_{1-42}$ (Aβ) levels, amyloid tracer uptake, and brain volumes.

Methods Twelve MS patients were recruited and divided according to their disease activity into active and non-active groups. All participants underwent neurological examination, neuropsychological testing, lumbar puncture, brain magnetic resonance (MRI) imaging, and ^{18}F-florbetapir PET. Aβ levels were determined in CSF samples from all patients. MRI and PET images were co-registered, and mean standardized uptake values (SUV) were calculated for each patient in the NAWM and in the DWM. To calculate brain volumes, brain segmentation was performed using statistical parametric mapping software. Nonparametric statistical analyses for between-group comparisons and regression analyses were conducted.

Results We found a lower SUV in DWM compared to NAWM ($p < 0.001$) in all patients. Decreased NAWM-SUV was observed in the active compared to non-active group ($p < 0.05$). Considering only active patients, NAWM volume correlated with NAWM-SUV ($p = 0.01$). Interestingly, CSF Aβ concentration was a predictor of both NAWM-SUV ($r = 0.79$; $p = 0.01$) and NAWM volume ($r = 0.81$, $p = 0.01$).

Conclusions The correlation between CSF Aβ levels and NAWM-SUV suggests that the predictive role of β-amyloid may be linked to early myelin damage and may reflect disease activity and clinical progression.

Keywords PET · Amyloid tracer · Florbetapir · Multiple sclerosis · Amyloid · White matter

Anna M. Pietroboni, Tiziana Carandini, Daniela Galimberti, and Giorgio Marotta contributed equally to this work.

✉ Anna M. Pietroboni
pb.anna@libero.it

1 Fondazione IRCCS Ca' Granda Ospedale Maggiore Policlinico, Via F. Sforza 35, 20122 Milan, Italy

2 University of Milan, Milan, Italy

3 Dino Ferrari Center, Milan, Italy

4 Neuroimaging Laboratory, IRCCS Santa Lucia Foundation, Rome, Italy

5 Department of Neurosciences, Psychology, Drug Research and Child Health (NEUROFARBA), University of Florence, Florence, Italy

6 Department of Neuroscience, Brighton and Sussex Medical School, University of Sussex, Brighton, UK

Introduction

Multiple sclerosis (MS) is the most common chronic inflammatory disease of the central nervous system (CNS) [1], whose demyelination is the pathological hallmark. MS is characterized by inflammation, axonal damage, and neurodegeneration [2]. The factors that promote spontaneous remyelination or determine axonal and neuronal loss remain poorly understood [3], and currently there are no reliable prognostic biomarkers of disease progression.

Magnetic resonance imaging (MRI) is the most widely used technique for identifying the demyelinating lesions, especially in the white matter (WM). However, no strong correlation exists between conventional MRI measures, such as T2- and T1-weighted lesion loads, and risk of disease progression,

and no MRI technique is currently specific enough to assess myelin damage and repair in vivo [4–6].

Positron emission tomography (PET) with amyloid tracers (e.g. Pittsburgh compound B, florbetapir, florbetaben, flutemetamol) was originally developed for imaging of amyloid deposition in neurodegenerative disorders and dementia [7], but it has recently been repurposed as an imaging marker for quantification of myelin loss and repair in MS [5, 8–10]. Amyloid tracers bind extensively to WM, and its uptake decreases with demyelination [8]. The usefulness of amyloid tracers in MS is traditionally considered secondary to their nonspecific binding to WM, possibly being trapped in β-sheet structures of myelin proteins or being highly soluble in the myelin-associated lipid bilayer [10, 11]. Nevertheless, emerging evidence supports a connection between amyloid and myelin pathology. Acute WM lesions show reduced amyloid tracer uptake compared with normal-appearing WM (NAWM), reflecting more extensive myelin loss in the lesions than in the NAWM [9, 10, 12, 13]. Additionally, in patients with relapsing-remitting (RR) MS, increased uptake within the lesions was found to be associated with a more benign clinical evolution [9]. In light of these data, amyloid PET tracers may represent a new tool for monitoring MS progression and providing outcome measures [8]. Amyloid PET tracer WM uptake in MS has raised questions about its utility as a biomarker of demyelination. Moreover, amyloid precursor protein (APP) accumulates in damaged axons in MS [14, 15], suggesting that it may constitute a reliable marker of axon demyelination. High APP immunoreactivity has been found in actively demyelinating MS lesions but not in chronic lesions, indicating a peculiar modification of APP metabolism across disease stages [16]. Moreover, β-amyloid (Aβ) may be involved in remyelination: the β-site APP-cleaving enzyme 1 (BACE1), the enzyme that processes APP to generate Aβ, is also involved in the cleavage of neuregulin 1, a protein that plays a crucial role in oligodendrocyte differentiation and remyelination. Indeed, the genetic deletion of BACE1 during development leads to hypomyelination [17]. Several studies have aimed to determine how remyelination and MS are affected by APP and the proteins expressed via APP proteolytic processing, and whether amyloid PET can provide an in vivo molecular diagnosis of this process, but the question is still open.

Reduced cerebrospinal fluid (CSF) Aβ levels have been reported in MS patients [18–22] and have recently been suggested as a prognostic biomarker [22, 23].

Given these premises, the aim of the current study is twofold: (1) to assess amyloid tracer uptake in damaged WM (DWM) and NAWM of MS patients divided according to their disease activity, and (2) to investigate possible correlations between amyloid tracer uptake and CSF Aβ levels, WM brain volumes, and clinical markers of disease progression.

Materials and methods

Subjects

Twelve patients with a diagnosis of MS according to the 2010 revised McDonald criteria were recruited [24]. Seven patients had RR-MS, three patients had secondary progressive (SP) subtype, and two patients had primary progressive (PP) MS. The patients were then divided according to their disease activity in the last year before recruitment [25]: eight patients were considered active (active MS) based on clinical relapse and/or MRI findings (contrast-enhancing lesions, new or unequivocally enlarging T2 lesions), whereas four patients were deemed stable, with no evidence of acute inflammation (non-active MS). The main demographic and clinical characteristics of all recruited subjects are summarized in Table 1.

All patients underwent clinical assessment, neuropsychological evaluation, brain MRI, ^{18}F-florbetapir PET, and lumbar puncture (LP). LP was always performed before starting any treatment (i.e. corticosteroids). All patients underwent brain MRI for diagnostic purposes and ^{18}F-florbetapir PET within a maximum of 4 weeks after brain MRI. For each recruited patient, we assessed the Expanded Disability Status Scale (EDSS) score [26] and we calculated the Bayesian Risk Estimate for MS at Onset (BREMSO). The BREMSO score was created in order to assess an individual risk score calculated from demographic and clinical variables collected at disease onset: the higher the BREMSO score, the higher the risk of future disability [27].

The neuropsychological evaluation was assessed on the same day as the ^{18}F-florbetapir PET using the Italian translation of the Rao Brief Repeatable Battery (BRB-N) of Neuropsychological Tests in Multiple Sclerosis [28]. Tests were administered by a trained neuropsychologist in a standardized manner, during daytime, in a quiet room, and in a fixed order. The administration of the whole battery took about 30 min. The neuropsychological battery included the following: selective reminding test (SRT), consistent long-term retrieval (SRT-CLTR), spatial recall test, oral Symbol Digit Modalities Test (SDMT), Paced Auditory Serial Addition Test at 3 (PASAT3) and 2 s (PASAT2), selective reminding test–delayed recall (SRT-D), and spatial recall test-delayed. Neuropsychological tests included in the analyses were adjusted for age, gender, and/or education, according to the Italian validation study [28].

The current study was approved by the institutional review board of the Fondazione Cà Granda, IRCCS Ospedale Maggiore Policlinico (Milan, Italy). All MS patients gave their written informed consent for this research before entering the study.

Table 1 Clinical and demographic data for each recruited subject

Patient	Disease activity	Disease course	Age (years)	Gender	Disease duration (months)	EDSS score	BREMSO score
1	Active	RR-MS	23	F	26	3.0	2.06
2	Active	RR-MS	27	F	24	2.0	1.00
3	Active	RR-MS	20	M	17	1.5	0.42
4	Active	PP-MS	62	F	36	2.0	1.20
5	Active	RR-MS	25	M	15	1.0	0.42
6	Active	RR-MS	35	F	15	2.0	1.05
7	Active	RR-MS	27	F	60	2.5	−0.60
8	Active	SP-MS	29	M	84	6.5	2.12
9	Non-active	SP-MS	55	M	16	3.5	1.58
10	Non-active	RR-MS	40	F	32	3.0	2.35
11	Non-active	PP-MS	56	M	48	2.0	1.71
12	Non-active	RR-MS	34	F	21	1.0	1.67

EDSS Expanded Disability Status Scale score *BREMSO* Bayesian Risk Estimate for MS at Onset, *RR* relapsing-remitting, *PP* primary progressive, *SP* secondary progressive

CSF collection and Aβ determination

CSF samples were collected by LP in the L3/L4 or L4/L5 interspace. Following LP, CSF samples were centrifuged at 8000 rpm for 10 min. The supernatant was aliquoted in polypropylene tubes and stored at – 80 °C until use. CSF cell counts, glucose, and proteins were determined. Albumin was measured by rate nephelometry. Oligoclonal bands (OCB) were evaluated by isoelectric focusing. CSF Aβ was measured using a commercially available sandwich enzyme-linked immunosorbent assay (ELISA) kit (Fujirebio, Ghent, Belgium).

MRI acquisition

All patients underwent an MRI examination on an Achieva 3.0T scanner (Philips, Best, Netherlands). The protocol included the following: (1) a T1-weighted scan (Repetition Time (TR) 9.90 ms; Echo Time (TE) 4.61 ms; flip angle 8°; slices thickness 1 mm; gap 0), (2) fluid-attenuated inversion recovery (FLAIR) images (TR 11000 ms; TE 125 ms; flip angle 90°; slice thickness 1 mm; gap 0), and (3) a T2-weighted scan (TR 2492 ms; TE 78 ms; flip angle 90°; slice thickness 4 mm; gap 0).

PET acquisition

PET scans were obtained with a Biograph TruePoint 64 PET/CT scanner (Siemens, Erlangen, Germany). All patients underwent ^{18}F-florbetapir PET scanning at rest after intravenous injection of 370 MBq. Patients were positioned comfortably in a quiet room for at least 50 min. Each acquisition included a CT transmission scan of the head (55 mAs lasting 10 s) followed by a 20-min PET list-mode acquisition. PET sections were reconstructed with four 5-min frames to verify the absence of patient movement during the acquisition, and then with one frame of all 20 min in the form of transaxial images of 168 × 168 pixels (2 mm), using the iterative 3D TrueX algorithm with eight iterations and 14 subsets, with a Gaussian filter with full width at half maximum of 4 mm, and corrected for scatter and for attenuation using density coefficients derived from the low-dose CT scan of the head obtained with the same scanner, using the proprietary software.

Neuroimaging data analysis

The statistical analyses were performed using statistical parametric mapping software (SPM12, Wellcome Centre for Human Neuroimaging, University College London, UK). Using the ImCalc function of SPM, standardized uptake value (SUV) PET maps were derived as SUV = AC/(radiotracer dose/BW), where AC represents the activity concentration in a given voxel (kBq/ml), the radiotracer dose is the injected florbetapir dose corrected for residual activity in the syringe (MBq), and BW is body weight (kg).

FLAIR images and SUV-PET images were co-registered to individual volumetric T1-weighted images.

To quantify the macroscopic WM lesion load, lesions were segmented using the lesion growth algorithm [29] as implemented in the Lesion Segmentation Tool (LST) toolbox version 2.0.15 (www.statistical-modelling.de/lst.html) for SPM. The algorithm first segments the T1 images into the main tissue classes. This information is then combined with the co-registered FLAIR intensities in order to calculate lesion belief maps. By thresholding these maps with a threshold K value of 0.2 (determined by visual inspection of the results for the patients), an initial binary lesion map is obtained, which is subsequently grown along voxels that appear hyperintense in

the FLAIR image, and the region of interest (ROI) for the DWM is created. For each dataset, the WM lesion load was calculated, visually inspected to exclude the presence of macroscopic artifacts, and used for correlation analyses.

Lesions in T1-weighted images were previously filled using the lesion-filling tool in the LST toolbox. The lesion-filled T1-series images were segmented according to GM, WM, and CSF tissue probability maps to generate the normalization deformation field into the Montreal Neurological Institute (MNI) space to be applied to the co-registered SUV-PET scans.

Using the WM and GM probability map of segmentation of the individual lesion-filled T1-images, we extracted the mean SUV for each patient's total WM by the co-registered SUV-PET images. To calculate the mean SUV of NAWM, the volume of interest (VOI) representing NAWM was calculated by subtracting the DWM VOI from the total WM VOI (Fig. 1).

GM was also evaluated using the Siemens *syngo*®.PET Amyloid Plaque quantification molecular imaging neurology software on the *syngo*.via client-server, using the cortical ROI of the anterior cingulate gyrus, orbital part of frontal lobe, superior parietal lobule, posterior cingulate gyrus, precuneus, and temporal lobe, and of the average of these six regions.

The whole cerebellum was used as the reference region for the standardized uptake value relative ratios (SUVR).

Finally, to obtain brain volumetrics, brain segmentation was performed using SPM12. For each scan, we derived the GM, total WM, NAWM, and DWM fractions, calculated as the ratio of GM, total WM, NAWM, and DWM volumes to total intracranial volume (TIV), respectively. Data were subsequently converted to percentages.

Statistical analysis

All statistical analyses were performed using SPSS 21.0 for Windows (IBM Corp., Armonk, NY, USA), GraphPad PRISM 6.0 (GraphPad Software, La Jolla, CA, USA), and SPM12.

Due to the non-normal distribution of data (as preliminarily assessed by the Shapiro-Wilk test), all between-group comparisons were tested by nonparametric inferential statistical analyses (Mann–Whitney *U* test and Wilcoxon test for paired *t* tests). We used a paired *t* test for the comparison of the amyloid tracer mean SUV between DWM and NAWM.

All correlation analyses were performed assessing the Pearson correlation coefficient. Linear regression analyses were performed with WM-SUV and NAWM volume as dependent variables and CSF Aβ levels as explanatory variable. Each regression model was adjusted in order to control for the potential effects of age and gender.

For all analyses, the statistical threshold was set to $p < 0.05$, except for correlation between NAWM-SUV and clinical assessment, which was set to $p < 0.025$ after Bonferroni correction for multiple comparisons ($\alpha = 0.05/2 = 0.025$), and for correlation between CSF Aβ levels and clinical assessment, which was set to $p < 0.016$ after Bonferroni correction for multiple comparisons ($\alpha = 0.05/3 = 0.016$).

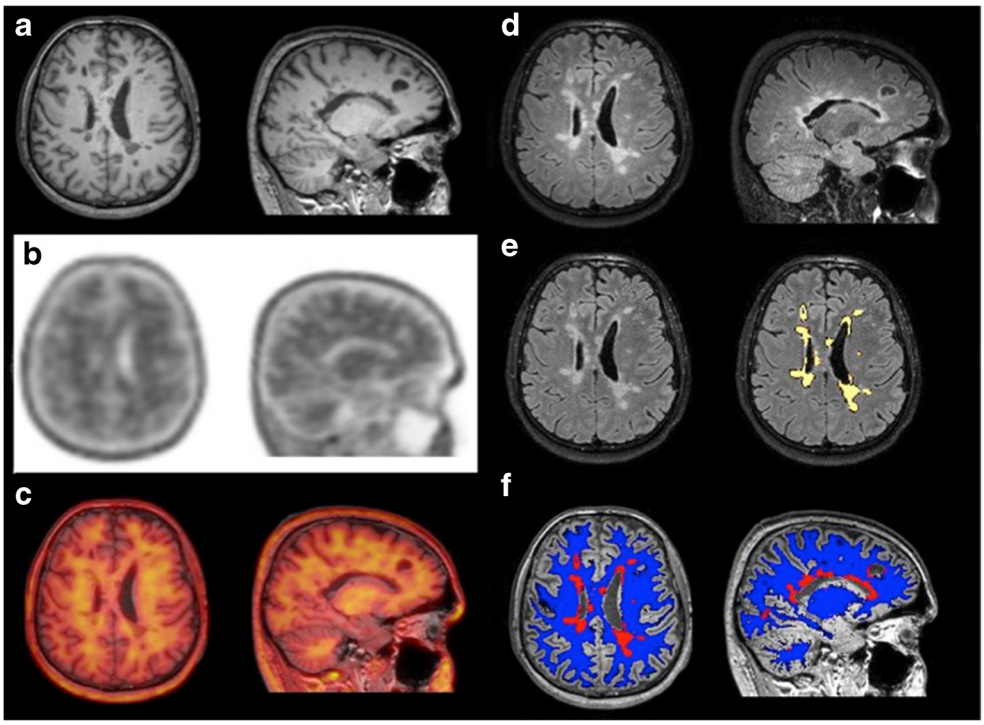

Fig. 1 **a** T1-weighted MRI; **b** co-registered ^{18}F-florbetapir PET and **c** T1-weighted MRI/PET fusion images (using the hot iron map); **d** T2-weighted FLAIR MRI; **e** lesion elaboration from the Lesion Segmentation Tool (yellow); **f** normal-appearing white matter (blue) and damaged white matter (red) segmentation on T2-weighted FLAIR MRI

Results

The main CSF, PET, and MRI findings are summarized in Tables 2 and 3.

Concerning the GM tracer uptake, all patients were categorized as amyloid-negative by quantitative cutoff because their GM-SUVR average was less than 1.10 [30]. No correlation was found between CSF Aβ levels and GM-SUVR average (for all SUVR see Table 3).

Concerning the WM tracer uptake, DWM-SUV was lower than NAWM-SUV (1.032 ± 0.112 vs. 1.128 ± 0.122; $p = 0.0005$; Fig. 2a) in each subject. Comparing patients according to their clinical course (RR vs. SP/PP), no differences in NAWM-SUV or DWM-SUV were observed. Conversely, when grouping patients according to their disease activity (active vs. non-active), we found a reduced NAWM-SUV in the active group compared to the non-active group (1.077 ± 0.119 vs. 1.231 ± 0.023; $p = 0.028$; Fig. 2b), whereas no significant differences in DWM-SUV were observed.

NAWM-SUV correlated with both total WM volume ($r = 0.73$; $p = 0.006$) and NAWM volume ($r = 0.82$; $p = 0.01$; Fig. 3), but not with DWM volume ($r = -0.45$; $p > 0.05$), in all MS patients.

Focusing on the active group, CSF Aβ levels were lower in patients with WM-SUV < 1.05 than in those with WM-SUV ≥ 1.05 (698.8 ± 32.57 vs. 1033 ± 226.4; $p = 0.029$; Fig. 4a). Neither DMW-SUV nor NAWM-SUV correlated with patient age. CSF Aβ levels correlated with NAWM-SUV ($r = 0.79$; $p = 0.017$; Fig. 4b): the lower the CSF Aβ concentration, the lower the tracer uptake in the NAWM. The linear regression analysis showed CSF Aβ levels as a predictor of NAWM-SUV ($r = 0.79$; $p = 0.01$). NAWM-SUV correlated with NAWM volume ($r = 0.82$; $p = 0.01$; Fig. 4c), but not with DWM volume ($r = -0.64$; $p > 0.05$). The multiple regression analysis showed NAWM volume as the best predictor of NAWM-SUV ($r = 0.87$; $p = 0.007$). CSF Aβ levels correlated with NAWM volume ($r = 0.81$; $p = 0.01$; Fig. 4d), but not with DWM volume ($r = -0.36$; $p > 0.05$). The multiple regression analysis revealed CSF Aβ levels as the best predictor of NAWM volume ($r = 0.81$; $p = 0.007$).

As regards clinical data, NAWM-SUV in active patients showed a trend towards significance in the correlation with BREMSO score ($r = -0.75$; $p = 0.03$), although the data did not remain statistically significant after Bonferroni correction.

CSF Aβ levels correlated with the PASAT2 test ($r = 0.85$; $p = 0.007$), whereas the correlations with BREMSO score ($r = -0.73$; $p = 0.04$), EDSS score ($r = -0.72$; $p = 0.04$), and PASAT3 test ($r = 0.71$; $p = 0.04$) were no longer significant after Bonferroni correction.

Discussion

In this study, we report WM-SUV data for amyloid PET in patients with active and non-active MS in order to investigate possible differences between the two groups. To the best of our knowledge, this is the first attempt to correlate CSF Aβ levels and amyloid PET in MS reported thus far.

In line with previous studies [9, 10], we find that the amyloid tracer uptake in the largest lesion of each patient is reduced compared to their NAWM, confirming the role of amyloid PET as a biomarker of myelin loss.

Table 2 Main variables for each recruited subject

Patient	Disease activity	CSF Aβ levels (pg/ml)	Total WM mean SUV	NAWM mean SUV	DWM mean SUV	Total WM volume* (%)	NAWM volume* (%)	DWM volume* (%)
1	Active	681	1,033	1,034	0,961	27,61	27,47	0,14
2	Active	748	1,165	1,165	1,059	29,49	29,46	0,03
3	Active	1037	1,099	1,099	1,036	31,03	30,78	0,25
4	Active	746	0,958	0,959	0,842	26,99	26,39	0,61
5	Active	1302	1,240	1,240	1,171	31,81	31,70	0,10
6	Active	694	0,988	0,988	0,923	27,98	27,90	0,08
7	Active	1046	1,206	1,206	1,041	32,97	32,88	0,08
8	Active	674	0,922	0,924	0,885	30,82	28,81	2,01
9	Non-active	838	1,257	1,263	1,032	33,42	32,39	1,03
10	Non-active	570	1,209	1,209	1,108	35,09	35,09	0,00
11	Non-active	756	1,232	1,232	1,207	31,12	31,92	0,20
12	Non-active	519	1,220	1,220	1,120	32,59	32,54	0,05

*Volumes are expressed as percentages, calculated as the ratio of total WM, NAWM, and DWM volume to total intracranial volume

Aβ: β-amyloid; SUV: standardized uptake value; WM: white matter; NAWM: normal-appearing white matter; DWM: damaged white matter

Table 3 Standardized uptake value ratios (SUVR) relative to cerebellum in gray matter (GM) of the anterior cingulate gyrus, frontal lobe, parietal lobe, posterior cingulate gyrus, precuneus, and temporal lobe, and the average of these six regions, and of total white matter (WM), normal-appearing WM (NAWM), and damaged WM (DWM) for each recruited subject

Patient	Disease activity	GM Anterior cingulate gyrus SUVR	GM Frontal lobe SUVR	GM Parietal lobe SUVR	GM Posterior cingulate gyrus SUVR	GM Precuneus SUVR	GM Temporal lobe SUVR	GM SUVR Average	Total WM SUVR	NAWM SUVR	DWM SUVR
1	Active	0,99	0,91	0,92	0,91	1,03	1,04	0,97	1,475	1,475	1,372
2	Active	0,89	0,83	0,91	0,93	0,84	1,05	0,91	1,417	1,417	1,288
3	Active	0,87	0,84	0,88	0,92	0,92	0,97	0,90	1,338	1,338	1,261
4	Active	0,94	0,74	0,85	0,91	0,78	0,98	0,87	1,322	1,324	1,163
5	Active	0,84	0,82	0,92	0,95	0,90	1,07	0,92	1,473	1,474	1,391
6	Active	0,93	0,84	0,88	0,92	0,94	1,11	0,94	1,541	1,541	1,440
7	Active	0,98	0,89	1,06	1,05	0,97	1,11	1,05	1,501	1,502	1,296
8	Active	0,87	0,92	0,97	0,98	1,01	1,02	0,96	1,431	1,434	1,373
9	Non-active	0,94	0,87	0,91	0,92	1,00	1,07	0,95	1,458	1,465	1,197
10	Non-active	1,02	0,94	0,97	1,03	0,99	1,12	1,01	1,482	1,482	1,359
11	Non-active	0,90	0,91	0,90	0,98	0,90	1,09	0,95	1,359	1,359	1,332
12	Non-active	1,12	0,92	1,07	1,04	0,98	1,18	1,05	1,591	1,591	1,461

Moreover, we show that ^{18}F-florbetapir uptake in patients with active disease is lower than that in non-active patients, suggesting an interesting link between early WM damage and disease activity. A previous study described a more marked reduction in amyloid tracer uptake in both DWM and NAWM in patients with progressive MS compared to RR-MS patients [10]. The authors speculated that such findings may be associated with the reduced remyelination present in the progressive forms of the disease [10, 31].

We find that active patients have lower amyloid tracer uptake than non-active patients, regardless of their disease form, and that the lower uptake is not only in the DWM but also in the NAWM.

The most interesting finding of our study is that the tracer uptake in the NAWM correlates with CSF Aβ levels: the lower the uptake, the lower the CSF Aβ concentration. We hypothesize that active patients, i.e. those with lower uptake in both DWM and NAWM and with lower CSF Aβ levels, may have a reduced capacity for remyelination and consequently a higher risk of disease progression. Strengthening this hypothesis, we also find lower uptake in the NAWM and lower CSF Aβ levels in those patients with smaller NAWM volume.

We recently described a relationship between low CSF Aβ levels and worse prognosis in MS [22, 23]. In line with these findings and the hypothesis [22], the correlation we describe between amyloid tracer uptake and CSF Aβ concentration suggests that amyloid plays a role in the progression of WM damage in MS. Thus, ^{18}F-florbetapir PET may represent a marker of early WM damage and a useful prognostic tool. As part of this speculation, we had already hypothesized that lower CSF Aβ levels could be associated with a decreased ability for remyelination of CNS axons, with early WM and GM damage, resulting in a higher probability of disease progression [22]. Nevertheless, the exact role played by Aβ remains to be determined. Further studies are necessary to draw a definitive picture.

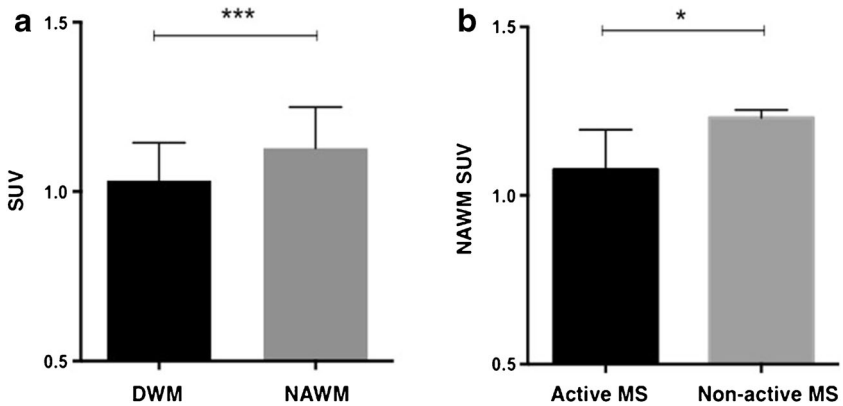

Fig. 2 **a** Comparison of the amyloid tracer mean standard uptake value (SUV) in damaged white matter (DWM) and normal-appearing white matter (NAWM) of all patients ($p = 0.0005$). **b** Comparison of the amyloid tracer mean SUV in the NAWM of active and non-active patients ($p = 0.028$)

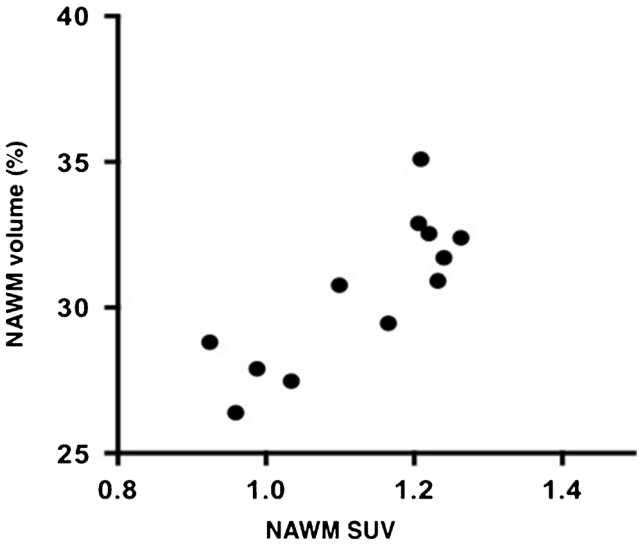

Fig. 3 Correlation between the normal-appearing white matter (NAWM) amyloid tracer mean standard uptake value (SUV) and NAWM volume in all patients. NAWM volume is expressed as a percentage, calculated as the ratio of NAWM volume to total intracranial volume ($r = 0.82$; $p = 0.01$)

There are some limitations when considering our study. First, we acknowledge that this represents an exploratory study and that a larger cohort of patients will be needed to confirm our findings. The number of patients included was unfortunately limited due to the removal of the radiopharmaceutical ^{18}F-florbetapir from the market in Europe in January 2018. Second, all patients underwent ^{18}F-florbetapir PET scanning following an acquisition protocol validated for patients with Alzheimer's disease (AD) to ensure the absence of movement during the acquisition. Our study did not aim to optimize the protocol for MS patients, but rather to apply the best protocol used to ^{18}F-florbetapir PET acquisition. Because all patients, including those with active disease, were very cooperative, and none of them moved their head during the entire acquisition protocol, the 20-min static images were used for all measurements.

In conclusion, this study provides evidence of the role of amyloid PET in the assessment of MS, particularly in relation to disease activity and early prognosis. Moreover, these findings suggest a predictive role for CSF Aβ levels in MS. A replication in a larger cohort of patients is required to confirm these preliminary data.

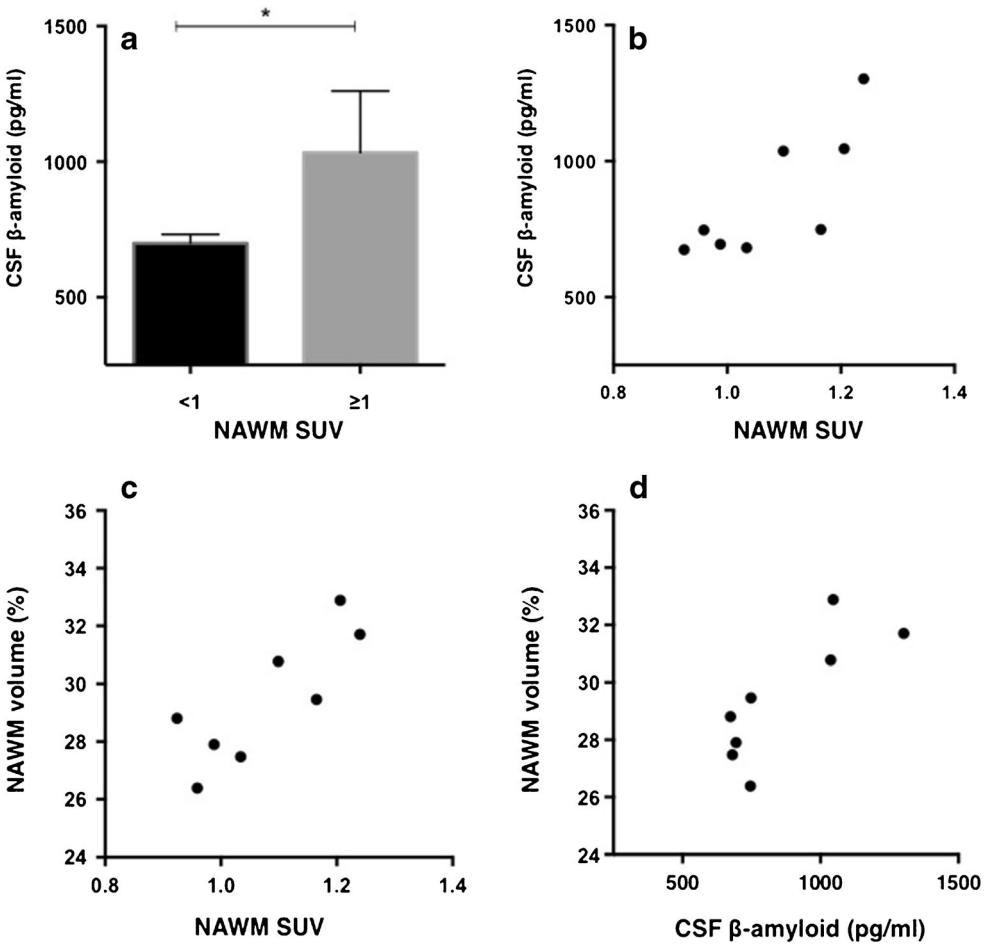

Fig. 4 **a** Comparison of CSF levels of β-amyloid in active patients according to their normal-appearing white matter (NAWM) amyloid tracer mean standard uptake value (SUV) ($p = 0.029$). **b** Correlation between the NAWM amyloid tracer mean SUV and the CSF levels of β-amyloid in active patients ($r = 0.79$; $p = 0.017$). **c** Correlation between the NAWM amyloid tracer mean SUV and the NAWM volume in active patients ($r = 0.82$; $p = 0.01$). **d** Correlation between CSF levels of β-amyloid and the NAWM volume in active patients ($r = 0.81$; $p = 0.01$). NAWM volume is expressed as percentage, calculated as the ratio of NAWM volume to total intracranial volume

Acknowledgements This research was supported by Fondazione Monzino and the Italian Ministry of Health ("Ricerca Corrente" to ES). GGF was supported by the Associazione Italiana Ricerca Alzheimer ONLUS (AIRAlzh Onlus)-COOP Italia.

Compliance with ethical standards

Conflict of interest The authors declare that they have no conflict of interest.

Statement of human rights All procedures performed in studies involving human participants were in accordance with the ethical standards of the institutional and/or national research committee and with the 1964 Helsinki declaration and its later amendments or comparable ethical standards.

Statement on the welfare of animals This article does not contain any studies with animals performed by any of the authors.

Informed consent Informed consent was obtained from all individual participants included in the study.

References

1. Reich DS, Lucchinetti CF, Calabresi PA. Multiple Sclerosis. N Engl J Med. 2018;378:169–80.
2. Lassmann H. Multiple sclerosis: Lessons from molecular neuropathology. Exp Neurol. 2014:2–7.
3. Franklin RJM, Ffrench-Constant C. Remyelination in the CNS: From biology to therapy. Nat Rev Neurosci. 2008:839–55.
4. Filippi M, Paty DW, Kappos L, Barkhof F, Compston DAS, Thompson AJ, et al. Correlations between changes in disability and T2-weighted brain MRI activity in multiple sclerosis: A follow-up study. Neurology. 1995;45:255–60.
5. Stankoff B, Freeman L, Aigrot MS, Chardain A, Dollé F, Williams A, et al. Imaging central nervous system myelin by positron emission tomography in multiple sclerosis using [methyl-11C]-2-(4-methylaminophenyl)- 6-hydroxybenzothiazole. Ann Neurol. 2011;69:673–80.
6. Bodini B, Louapre C, Stankoff B. Advanced imaging tools to investigate multiple sclerosis pathology. Presse Med. 2015:e159–e67.
7. Payoux P. Salabert AS. New PET markers for the diagnosis of dementia. Curr Opin Neurol. 2017:608–16.
8. Matías-Guiu JA, Oreja-Guevara C, Cabrera-Martín MN, Moreno-Ramos T, Carreras JL, Matías-Guiu J. Amyloid proteins and their role in multiple sclerosis. Considerations in the use of amyloid-PET imaging. Front Neurol. 2016.
9. Bodini B, Veronese M, García-Lorenzo D, Battaglini M, Poirion E, Chardain A, et al. Dynamic Imaging of Individual Remyelination Profiles in Multiple Sclerosis. Ann Neurol. 2016;79:726–38.
10. Matías-Guiu JA, Cabrera-Martín MN, Matías-Guiu J, Oreja-Guevara C, Riola-Parada C, Moreno-Ramos T, et al. Amyloid PET imaging in multiple sclerosis: an 18F-florbetaben study. BMC Neurol. 2015;15:243.
11. Grecchi E, O'Doherty J, Veronese M, Tsoumpas C, Cook GJ, Turkheimer FE. Multimodal Partial-Volume Correction: Application to 18F-Fluoride PET/CT Bone Metastases Studies. J Nucl Med. 2015;56:1408–14.
12. Glodzik L, Kuceyeski A, Rusinek H, Tsui W, Mosconi L, Li Y, et al. Reduced glucose uptake and Aβ in brain regions with hyperintensities in connected white matter. Neuroimage. 2014;100:684–91.
13. Glodzik L, Rusinek H, Li J, Zhou C, Tsui W, Mosconi L, et al. Reduced retention of Pittsburgh compound B in white matter lesions. Eur J Nucl Med Mol Imaging. 2015;42:97–102.
14. Mangiardi M, Crawford DK, Xia X, Du S, Simon-Freeman R, Voskuhl RR, et al. An animal model of cortical and callosal pathology in multiple sclerosis. Brain Pathol. 2011;21:263–78.
15. Trapp BD, Peterson J, Ransohoff RM, Rudick R, Mörk S, Bö L. Axonal Transection in the Lesions of Multiple Sclerosis. N Engl J Med. 1998;338:278–85.
16. Gehrmann J, Banati RB, Cuzner ML, Kreutzberg GW, Newcombe J. Amyloid precursor protein (APP) expression in multiple sclerosis lesions. Glia. 1995;15:141–51.
17. Hu X, Hicks CW, He W, Wong P, MacKlin WB, Trapp BD, et al. BACE1 modulates myelination in the central and peripheral nervous system. Nat Neurosci. 2006;9:1520–5.
18. Augutis K, Axelsson M, Portelius E, Brinkmalm G, Andreasson U, Gustavsson MK, et al. Cerebrospinal fluid biomarkers of β-amyloid metabolism in multiple sclerosis. Mult Scler J. 2013;19:543–52.
19. Mattsson N, Axelsson M, Haghighi S, Malmeström C, Wu G, Anckarsäter R, et al. Reduced cerebrospinal fluid BACE1 activity in multiple sclerosis. Mult Scler. 2009;15:448–54.
20. Mori F, Rossi S, Sancesario G, Codecá C, Mataluni G, Monteleone F, et al. Cognitive and cortical plasticity deficits correlate with altered amyloid-B CSF levels in multiple sclerosis. Neuropsychopharmacology. 2011;36:559–68.
21. Gentile A, Mori F, Bernardini S, Centonze D. Role of amyloid-beta CSF levels in cognitive deficit in MS. Clin Chim Acta. 2015;449:23–30.
22. Pietroboni AM, Schiano Di Cola F, Scarioni M, Fenoglio C, Spanò B, Arighi A, et al. CSF β-amyloid as a putative biomarker of disease progression in multiple sclerosis. Mult Scler. 2017;23:1085–91.
23. Pietroboni AM, Caprioli M, Carandini T, Scarioni M, Ghezzi L, Arighi A, et al. CSF β-amyloid predicts prognosis in patients with multiple sclerosis. Mult Scler J. 2018:135245851879170.
24. Polman CH, Reingold SC, Banwell B, Clanet M, Cohen JA, Filippi M, et al. Diagnostic criteria for multiple sclerosis: 2010 Revisions to the McDonald criteria. Ann Neurol. 2011;69:292–302.
25. Lublin FD, Reingold SC, Cohen JA, Cutter GR, Sørensen PS, Thompson AJ, et al. Defining the clinical course of multiple sclerosis: The 2013 revisions. Neurology. 2014:278–86.
26. Kurtzke JF. Rating neurologic impairment in multiple sclerosis: An expanded disability status scale (EDSS). Neurology. 1983;33:1444.
27. Bergamaschi R, Montomoli C, Mallucci G, Lugaresi A, Izquierdo G, Grand'Maison F, et al. BREMSO: A simple score to predict early the natural course of multiple sclerosis. Eur J Neurol. 2015;22:981–9.
28. Goretti B, Patti F, Cilia S, Mattioli F, Stampatori C, Scarpazza C, et al. The Rao's Brief Repeatable Battery version B: Normative values with age, education and gender corrections in an Italian population. Neurol Sci. 2014;35:79–82.
29. Schmidt P, Gaser C, Arsic M, Buck D, Förschler A, Berthele A, et al. An automated tool for detection of FLAIR-hyperintense white-matter lesions in Multiple Sclerosis. Neuroimage. 2012;59:3774–83.
30. Fleisher AS, Chen K, Liu X, Roontiva A, Thiyyagura P, Ayutyanont N, et al. Using positron emission tomography and florbetapir F18 to image cortical amyloid in patients with mild cognitive impairment or dementia due to Alzheimer disease. Arch Neurol. 2011;68:1404–11.
31. Mahad DH, Trapp BD, Lassmann H. Pathological mechanisms in progressive multiple sclerosis. Lancet Neurol. 2015;14:183–93.